STABILITY STUDY OF FRANCIS PUMP-TURBINE AT RUNAWAY

Christophe NICOLET*
Power Vision Engineering Sàrl, Switzerland

Sébastien ALLIGNÉ
Laboratory for Hydraulic Machines, EPFL, Switzerland

Basile KAWKABANI
Laboratory of Electrical Machines, EPFL, Switzerland

Jiri KOUTNIK
Voith Hydro Holding GmbH & Co. KG, Germany

Jean-Jacques SIMOND
Laboratory of Electrical Machines, EPFL, Switzerland

François AVELLAN
Laboratory for Hydraulic Machines, EPFL, Switzerland

ABSTRACT

This paper presents a numerical simulation study of an unstable behavior at runaway for a 2x350MW pump-turbine power plant. Unstable operation at runaway with a period of 15 seconds is properly simulated using a 1-dimensional approach. The simulation results points out a switch after 200 seconds of the unstable behavior between a period of oscillations initially of 15 seconds to a period of oscillation of 2.5 seconds corresponding to the hydraulic circuit first natural period. This phenomenon is described as a switch between a rigid and an elastic water column oscillation mode. The switch phenomenon is investigated by means of eigenvalues and eigenmodes analysis of the entire hydraulic system including rotating inertias and also through time domain simulations.

KEYWORDS: Transient behavior, runaway, instabilities, oscillation modes.

1 INTRODUCTION

Abnormal operation of Francis pump-turbines at runaway resulting from guide vanes servomotor failure is standard case investigated during transient analysis [12], [4]. Due to the S-shape of pump-turbines characteristics in turbine mode [13], the operation at runaway usually leads to unstable behavior characterized by a large period of oscillations typically between 8 to 20 seconds, corresponding to the so called hydromechanical mode. The period of the hydromechanical mode depends on the rotating inertias, the penstock water inertia and on the local gradient of the turbine characteristic in the S-shape as it is well described by Martin [7], [8]. The analytical prediction of the period of the oscillations at runaway provided by Martin was validated by Dörfler *et al.* by measurements made during speed no load operation on the prototype of a Francis pump-turbine [3]. However, during these tests, a lower period oscillation phenomenon was observed and described as the medium frequency unstable

* *Corresponding author:* Power Vision Engineering sàrl, phone: +41 21 691 45 13, fax: +41 21 691 45 13, email: christophe.nicolet@powervision-eng.ch

mode and it was noticed that the phenomenon was oscillating at a period close to the period of the first natural period of the piping system.

This paper presents a numerical simulation study of the transient behavior of a 2x340MW pump-turbine power plant, where the results show an unstable behavior at runaway. First, the modeling of hydraulic components based on equivalent scheme representation is presented. Then, the test case is described. The simulation results of the emergency shutdown of the 2 units considering a servomotor failure on the Unit 1, while the guide vanes of the unit 2 are closed normally are presented. Unstable operation of Unit 1 at runaway with a period of 15 seconds is properly simulated using the 1-dimensional approach. The simulation results points out a switch after 200 seconds of the unstable behavior between a period of oscillations initially of 15 seconds to a period of oscillation of 2.16 seconds corresponding to the hydraulic circuit first natural period. This phenomenon is described as a switch between a rigid and an elastic water column oscillation mode. The switch phenomenon is investigated by means of eigenvalues and eigenmodes analysis of the entire hydraulic system including rotating inertias and also through time domain simulations.

2 MODELING OF HYDRAULIC COMPONENTS

By assuming uniform pressure and velocity distributions in the cross section and neglecting the convective terms, the one-dimensional momentum and continuity balances for an elementary pipe filled with water of length *dx*, cross section *A* and wave speed *a*, see Fig. 1, yields to the following set of hyperbolic partial differential equations [16]:

$$\begin{cases} \dfrac{\partial h}{\partial t} + \dfrac{a^2}{gA} \cdot \dfrac{\partial Q}{\partial x} = 0 \\ \dfrac{\partial h}{\partial x} + \dfrac{1}{gA} \cdot \dfrac{\partial Q}{\partial t} + \dfrac{\lambda |Q|}{2gDA^2} \cdot Q = 0 \end{cases} \tag{1}$$

The system (1) is solved using the Finite Difference Method with a 1st order centered scheme discretization in space and a scheme of Lax for the discharge variable. This approach leads to a system of ordinary differential equations that can be represented as a T-shaped equivalent scheme [5], [11], [15] as presented in Fig. 2. The RLC parameters of this equivalent scheme are given by:

$$R = \frac{\lambda \cdot |\overline{Q}| \cdot dx}{2 \cdot g \cdot D \cdot A^2} \qquad L = \frac{dx}{g \cdot A} \qquad C = \frac{g \cdot A \cdot dx}{a^2} \tag{2}$$

Where λ is the local loss coefficient. The hydraulic resistance R, the hydraulic inductance L, and the hydraulic capacitance C correspond respectively to energy losses, inertia and storage effects.

The model of a pipe of length *L* is made of a series of n_b elements based on the equivalent scheme of Fig. 2. The system of equations relative to this model is set-up using Kirchoff laws. The model of the pipe, as well as the model of valve, surge tank, Francis turbine, etc, are implemented in the EPFL software SIMSEN, developed for the simulation of the dynamic behavior of hydroelectric power plants, [9], [14]. The time domain integration of the full system is achieved in SIMSEN by a Runge-Kutta 4th order procedure.

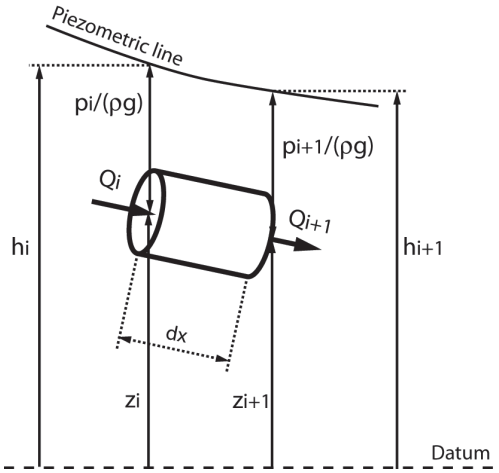

Fig. 1 Elementary hydraulic pipe of length dx.

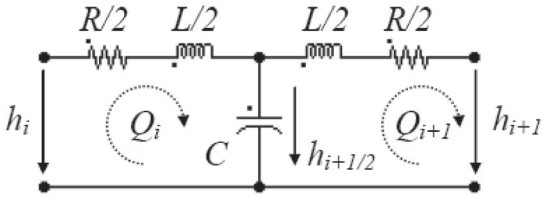

Fig. 2 Equivalent circuit of an elementary pipe of length dx.

As presented in Tab. 1, the modeling approach based on equivalent schemes of hydraulic components is extended to all the standard hydraulic components such as valve, surge tanks, air vessels, cavitation development, Francis pump-turbines, Pelton turbines, Kaplan turbines, pump, etc, see [9].

Component	Hydraulic scheme	Electrical equivalent scheme	Parameters
Generalized pipe	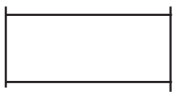	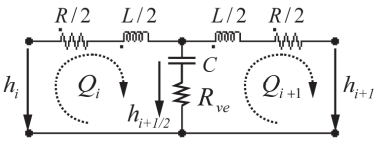	$R=\frac{dx\lambda\lvert Q\rvert}{2gDA^2}$ $R_{ve}=\frac{\mu}{\rho gAdx}$ $L=\frac{dx}{gA}$ $C=\frac{dxgA}{a^2}$
Valve	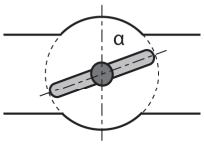	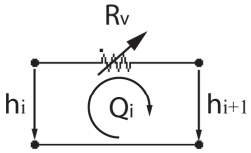	$R_v=\frac{K_v(\alpha)\lvert Q\rvert}{2gA^2}$
Surge tank	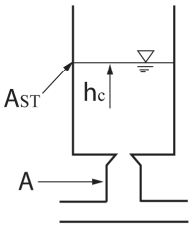	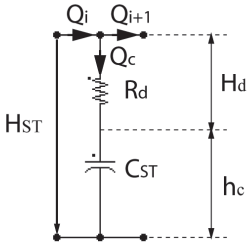	$R_d=\frac{K_d(Q)\lvert Q\rvert}{2gA^2}$ $C_{ST}=A_{ST}(h_c)$
Francis pump-turbine	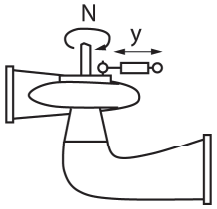	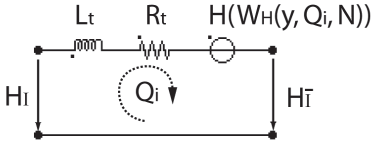	$H=H(W_H(y,Q,N))$ $T=T(W_B(y,Q,N))$ $R_t=R_t(W_H(y,Q,N))$ $L_t=\frac{l_{equ}}{gA}$

V_g : volume of gas [m³] W_H : turbine head characteristic [-] l_{equ} : turbine equivalent length [m]
h_g : pressure of gas [m] W_B : turbine torque characteristic [-] μ : viscosity of the fluid or material [Pa·s]

Tab. 1 Modeling of hydraulic components with related equivalent schemes.

3 CASE STUDY

The test case presented in Fig. 3 comprises an upper reservoir, a 1100 meters long gallery, a surge tank with constant cross section A_u=180m^2, a penstock of 975 meters feeding two Francis pump-turbines of 340 MW connected to a downstream surge tank of A_d=300m^2, and a 2500 meters long tailrace water tunnel. The rated parameters of the pump turbines are given in Tab. 2.

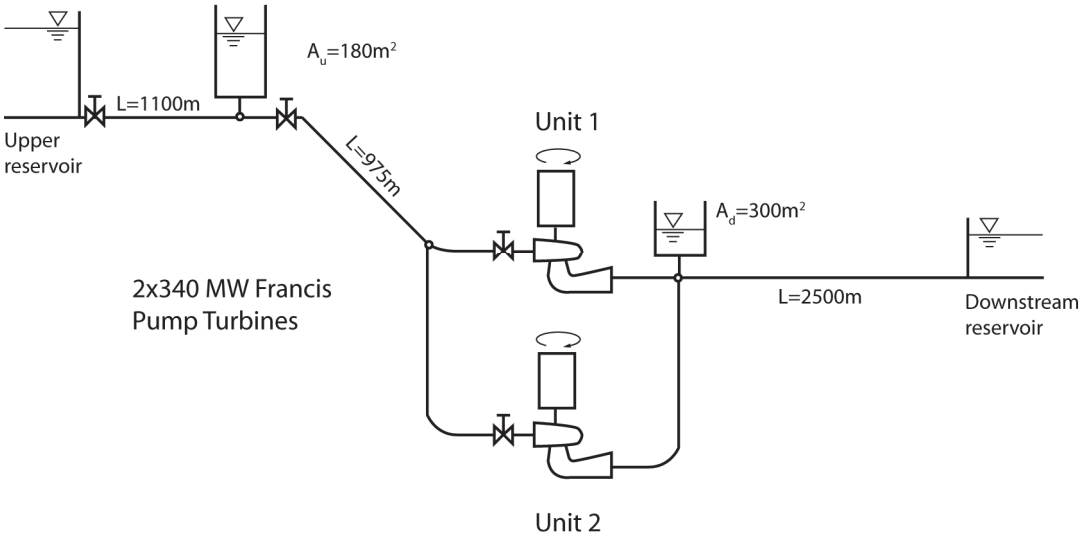

Fig. 3 Case study layout.

H_R [m]	Q_R [m^3/s]	N_R [rpm]	P_R [MW]	ν [-]	J [Kgm^2]
440	86	428.6	340	0.26	$1.5 \cdot 10^6$

Tab. 2 Rated values of the pump-turbine of Fig. 3.

4 EMERGENCY SHUTDOWN IN GENERATING MODE

The transient behavior of the power plant of Fig. 3 is simulated with SIMSEN for the case of an emergency shutdown of the two units operating close to the nominal operating point. A servomotor failure of Unit 1 is considered while the guide vanes of Unit 2 are closed linearly. The resulting transient behavior of Units 1 and 2 are presented respectively in Fig. 4 and Fig. 5.

Short term transient: 0 to 100 seconds

The Unit 2 is experiencing runaway that is reduced by the guide vane closure, while Unit 1, that have constant guide vane opening, is experiencing unstable operation at runaway due to the S-shape of the turbine characteristics inducing rotational speed, head, discharge and torque oscillation with a period of 15 seconds. Fig. 4, right, shows the operating point trajectory in the planes N_{11}-Q_{11} and N_{11}-T_{11} of the Unit 1 evidencing the S-shape of the turbine characteristic. Where N_{11}, Q_{11}, T_{11} are respectively the speed, discharge and torque factors given by:

$$N_{11} = \frac{N \cdot D_{ref}}{\sqrt{H}} \quad ; \quad Q_{11} = \frac{Q}{D_{ref}^2 \cdot \sqrt{H}} \quad ; \quad T_{11} = \frac{T}{D_{ref}^3 \cdot H} \tag{3}$$

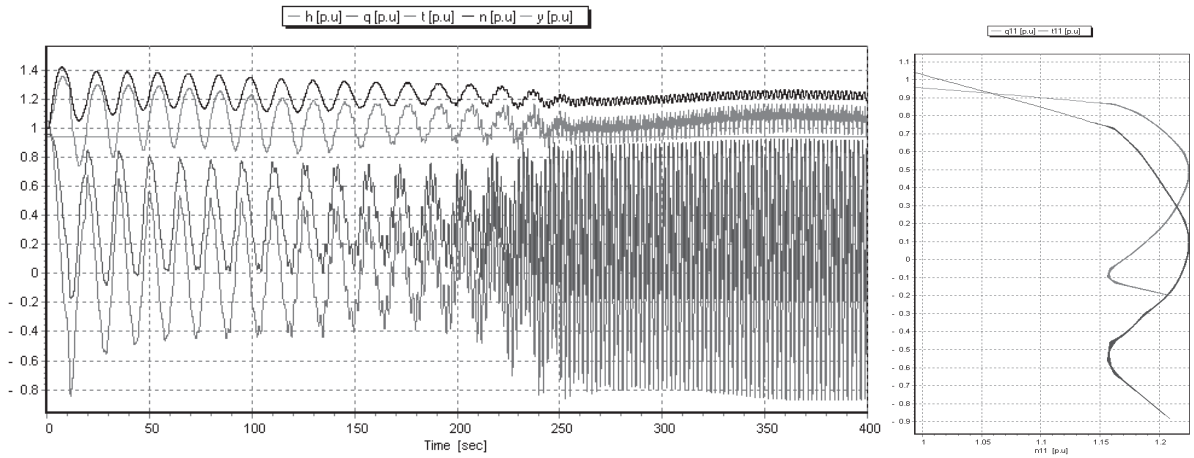

Fig. 4 Transient behavior of Unit 1 during emergency shutdown with servomotor failure (left) and related operating point trajectory in the plane N11-Q11 and N11-T11 (right).

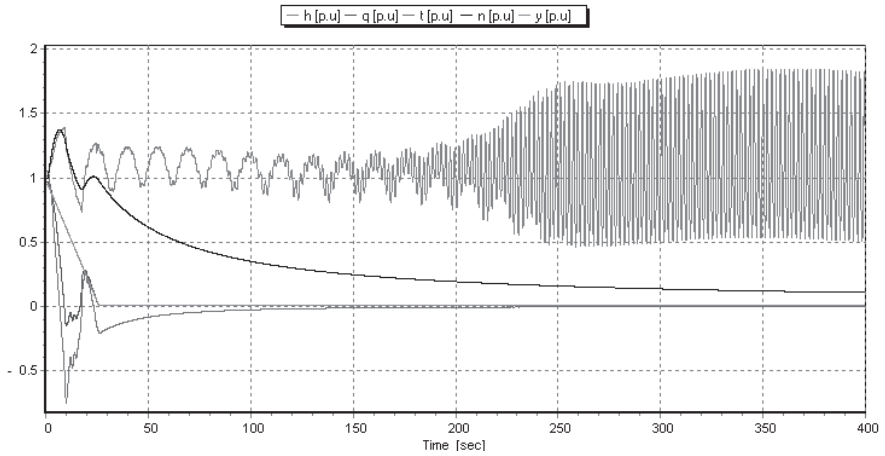

Fig. 5 Transient behavior of Unit 2 during emergency shutdown.

The runaway instability of Unit 1 corresponds to the so-called hydro-mechanical mode or rigid water column mode described by Martin [7], [8] which period depends on the total shaft line inertia J_{tot}, including the rotor, the shafts and the turbine itself, the penstock water inertia and on the turbine's characteristic. Let introduce the pump-turbine mechanical time constant τ_m and the penstock hydraulic time constant τ_h as follows:

$$\tau_m = \frac{J_{tot} \cdot \omega_R}{T_R} \qquad \tau_h = \frac{l_{pen}}{g \cdot A_{pen}} \cdot \frac{Q_R}{H_R} \tag{4}$$

The period of the rigid water column mode is given by [7]:

$$T_{RW} = \pi \cdot \sqrt{2 \cdot \frac{\tau_m \cdot \tau_h}{b1}} = 13.4 \text{ s} \tag{5}$$

Where *b1* is the slope of the turbine characteristic in the plane $\left(T/T_R\right)/\left(\omega/\omega_R\right)^2 = f\left(\left(Q/Q_R\right)/\left(\omega/\omega_R\right)\right)$. For the test case of Fig. 3, it gives, $\tau_m = 8.88$ s and $\tau_h = 1.07$ s, with b1=1.04.

The theoretical period of the rigid water column mode agrees well with the period obtained by simulation of T_{RW}=15s. The difference between the period obtained from the simulation and the period obtained from the linearized theory is due to the fact that the amplitude of the oscillations are above "small perturbation amplitudes", and consequently non-linearities influence the oscillation period.

Long term transient: 100 to 800 seconds

The emergency shutdown of the Units leads to a reduction of the discharge in the hydraulic system and consequently initiates upstream and downstream mass oscillations. The time evolution of the upstream and downstream water levels is presented in Fig. 6, pointing out the 2 different mass oscillations periods.

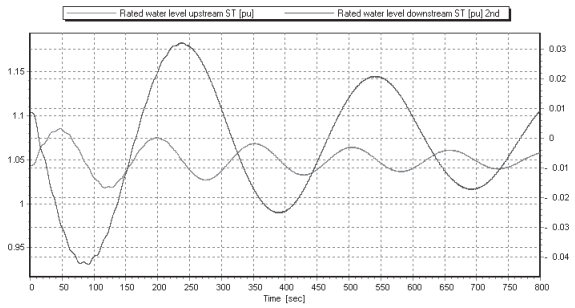

Fig. 6 Time evolution of the surge tanks rated water levels.

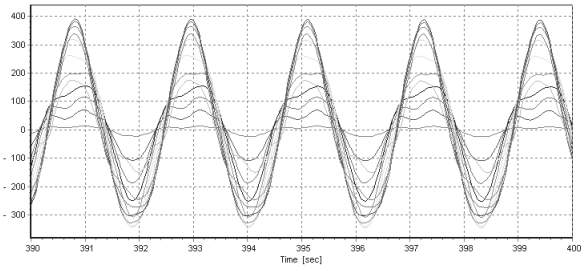

Fig. 7 Time evolution of the head along the penstock.

The most interesting point of the long term transient is the change of the behavior of the system instabilities that occurs between 100 seconds and 250 seconds. As presented in Fig. 4, it can be seen that the amplitudes of rotational speed and head of Unit 1 are decreasing while the amplitudes of the discharge and torque oscillations are strongly increasing, and the period of the oscillations is reduced to T_{EW}=2.16s. In the same time, the head of the Unit 2 is oscillating at the same period and exhibits peak-to-peak oscillation amplitudes of 1.3 times the rated head. Fig. 7 presents the time evolution of the head along the penstock for different locations pointing out pressure fluctuations of peak-to-peak amplitudes of 1.7 times the rated head in the middle of the penstock. The period of oscillation corresponds to the first natural frequency of the piping that can be calculated according to the total piping length comprised between the 2 surge tanks L_{tot} and the mean wave speed $\bar{a}$ and gives:

$$f_o = \frac{a}{\lambda} = \frac{\bar{a}}{2 \cdot L_{tot}} = \frac{1151}{2 \cdot 1243} = 0.463\text{Hz} \rightarrow T_{EW} = 2.16\text{s} \qquad (6)$$

Consequently, the oscillation mode with a period of 2.16s that arises after 250 seconds corresponds to the first natural frequency of the piping system which is excited by the turbine unstable behavior and dominates the rigid water column mode. This oscillation mode that involves the first piping natural frequency and the turbine is called elastic water column mode and was already observed on measurements by Dörfler *et al.* [3]. The difference in the denomination of the 2 modes lies to the fact that the rigid water column mode involves only inertias effects while the elastic column mode involves the compressibility effects of the piping system [6].

5 OSCILLATION MODES CHARACTERIZATIONS WITH TIME DOMAIN SIMULATION

To characterize better the differences between the rigid and the elastic water column oscillation modes, the head along the piping system between the upstream and downstream surge tanks are represented for two different time during one period of oscillation for the rigid mode in Fig. 8 and for the elastic mode in Fig. 9, for more details see also [10].

From Fig. 8, one can notice that rotational speed and head are oscillating in phase and torque and discharge are oscillating also in phase, but with a shift of 90° compared to head and rotational speed oscillations. The kinetic energy of the fluid is converted into angular kinetic energy of the mechanical inertias. The head amplitudes along the pipe appear to increase proportionally along the piping from the upstream surge tank until the turbine of Unit 1.

From Fig. 9, it can be seen that the amplitudes along the piping are drastically increased, as it corresponds to 1.7 times the rated head, and corresponds to the piping first natural mode shape. For the time t_o, it can be noticed that the amplitudes are not equal to zero as it is for the rigid mode. This is due to the second natural mode shape of the piping system that is also excited but features lower amplitudes than the first natural mode shape.

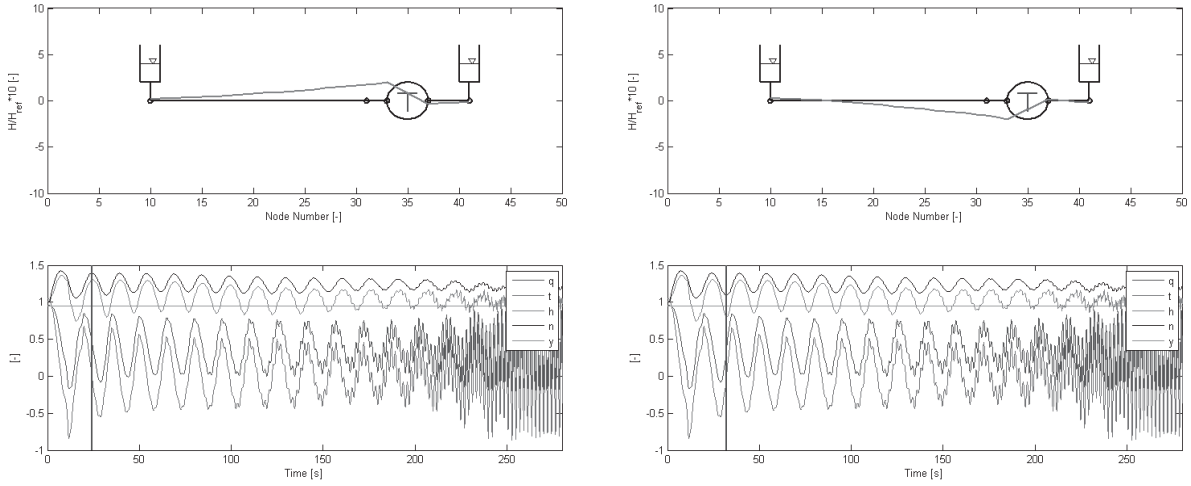

$t = t_o + T_{RW}/4$ $\qquad$ $t = t_o + 3 \cdot T_{RW}/4$

Fig. 8 Rigid water column mode.

It should be mentioned that for real emergency shutdown, the elastic water column mode would not have time to arise as there is closure of the protection valves for emergency shutdown. Typically, the main inlet valves are closing in 40 - 60 s and intake gate is closing in 120 - 180 s.

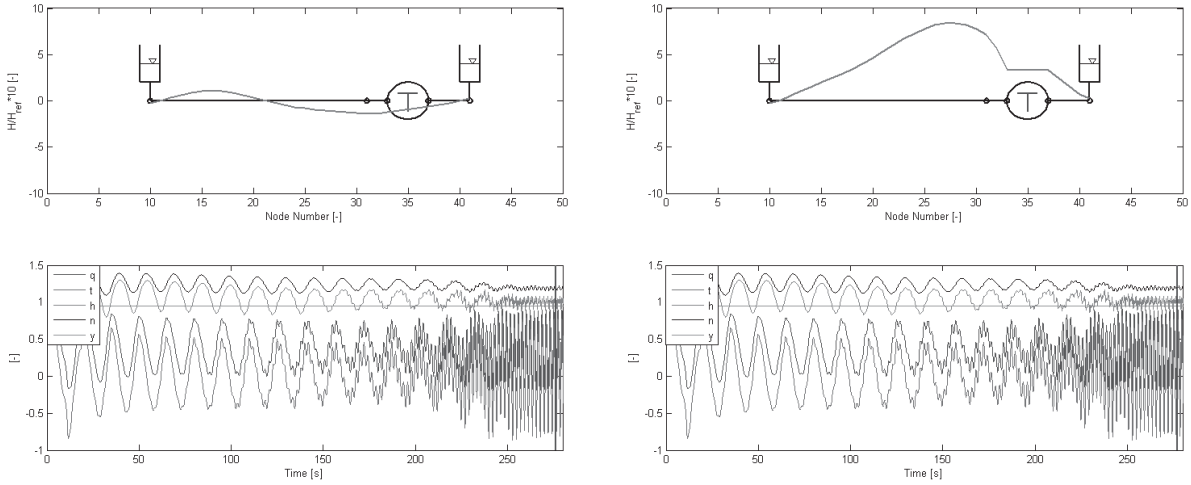

$t = t_o$ $\qquad\qquad$ $t = t_o + T_{EW}/4$

Fig. 9 Elastic water column mode.

6 OSCILLATION MODES CHARACTERIZATIONS WITH EIGENVALUES-EIGENMODES ANALYSIS

Hydraulic system eigenvalue analysis

The system of equations describing the dynamic behavior of the case study can be written as a first order differential equation set in the matrix form and can be linearized as follows:

$$[A]\cdot\frac{d\vec{x}}{dt}+\left[B\left(\vec{x}\right)\right]\cdot\vec{X}=\vec{C}\left(\vec{x}\right) \quad \xrightarrow{linearization} \quad [A]\cdot\frac{d\cdot\delta\vec{x}}{dt}+[B_l]\cdot\delta\vec{x}=\vec{0} \qquad (7)$$

The eigenvalues $s_k = \sigma_k + j\omega_k$ of the system (7) can be calculated from the characteristic equation of the system $\det\left(\left[I\right]\cdot s+\left[A\right]^{-1}\cdot\left[B_l\right]\right)=0$. Example of a complex eigenvalue and its complex conjugate is presented in Fig. 10. The real part corresponds to the damping σ while the imaginary part corresponds to the oscillation pulsation ω. Negative real part reveals stable behavior and positive real part reveals unstable behavior.

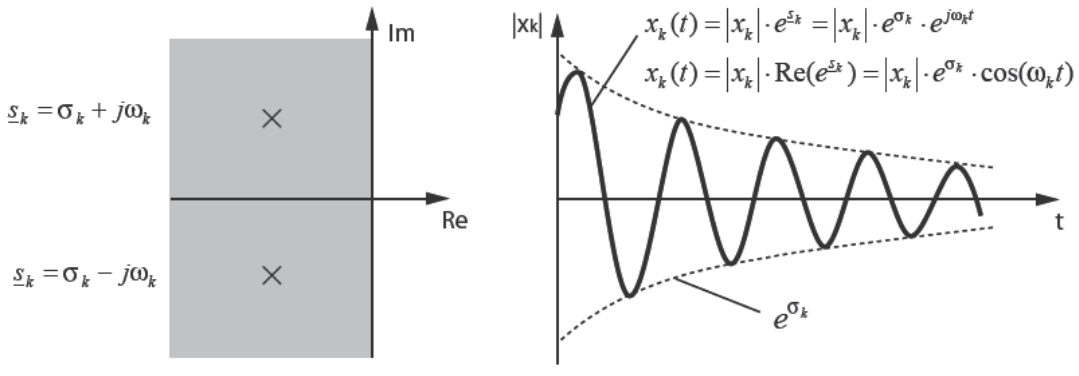

Fig. 10 Complex eigenvalue with complex conjugate.

An eigenvalues and eigenmodes computation module has been implemented in the simulation software SIMSEN [1] and enables to carry out modal analysis of hydraulic system featuring arbitrary topology, including elastic and viscoelatic pipes, surge tanks, air vessels, Francis pump-turbines including rotating inertias and PID turbine speed governors. This module will be extended in the future to Pelton and Kaplan turbines and to electrical systems.

Pump-turbine linearized model

The non-linear equation set which can be derived for the turbine gives:

$$\begin{bmatrix} L_t & 0 \\ 0 & J_t \end{bmatrix} \cdot \frac{d}{dt} \cdot \begin{pmatrix} Q \\ \omega \end{pmatrix} + \begin{bmatrix} R_t & 0 \\ 0 & 0 \end{bmatrix} \cdot \begin{pmatrix} Q \\ \omega \end{pmatrix} = \begin{pmatrix} -H_t + H_I - H_{\bar{I}} \\ T_t - T_{elec} \end{pmatrix} \tag{8}$$

The pump-turbine head H_t and torque T_t can be linearized as function of the turbine state variables Q, ω and y as follows [1], [2]:

$$\delta H_t(Q,\omega,y) = H_{t0} + \left.\frac{\partial H_t}{\partial Q_i}\right|_0 \cdot \delta Q + \left.\frac{\partial H_t}{\partial \omega}\right|_0 \cdot \delta\omega + \left.\frac{\partial H_t}{\partial y}\right|_0 \cdot \delta y \tag{9}$$

$$\delta T_t(Q,\omega,y) = T_{t0} + \left.\frac{\partial T_t}{\partial Q_i}\right|_0 \cdot \delta Q + \left.\frac{\partial T_t}{\partial \omega}\right|_0 \cdot \delta\omega + \left.\frac{\partial T_t}{\partial y}\right|_0 \cdot \delta y \tag{10}$$

In case of constant guide vane opening, the linearized matrix of the pump-turbine is given by [1]:

$$[B_l]_{\text{turbine}} = \begin{bmatrix} 2R_t + \left.\frac{\partial H_t}{\partial Q_i}\right|_0 & \left.\frac{\partial H_t}{\partial \omega}\right|_0 \\ \left.\frac{\partial T_t}{\partial Q_i}\right|_0 & \left.\frac{\partial T_t}{\partial \omega}\right|_0 \end{bmatrix} \tag{11}$$

The global matrix system of the case study also takes into account matrices of surge tanks and pipes.

System eigenmodes and eigenvalues

For simplicity, the case study presented in Fig. 3 has been reduced for the eigenvalue analysis to a system with only one pump-turbine. The size of the matrix system is 242 and includes the piping system, the upstream and downstream surge tanks and the pump-turbine N°1 with its rotating inertia with constant guide vanes. The remarkable eigevalues and related pressure and discharge mode shapes of the case study are computed with SIMSEN and are summarized respectively in Tab. 3 and in Tab. 4.

A particular point is related to the fact that the computation of the eigenvalues corresponding to the initial conditions of the time domain simulation shown in Fig. 4 provides a rigid water column mode with real eigenvalue, *i.e.* non-oscillating mode. Therefore, as the transient behavior related to the rigid water column mode is relatively slow, the eigenvalues can be computed for different times during the transient behavior of the pump-turbine experiencing unstable runaway behavior. It appears that the rigid water column mode becomes oscillatory, *i.e.* the related eigenvalue changes from real to complex value, only after a given time between t=2.4s and 3.8s. Therefore, the eigenvalues and eigenmodes shapes of Tab. 3 and Tab. 4 are computed for the time t=3.8s in order to have an oscillatory rigid water column mode. The related oscillating period is T=11.89s. Tab. 3 and Tab. 4 show that the eigenvalues and eigenmodes analysis provides: (i) the upstream and downstream mass oscillations, see N°1 and 2, (ii) the penstock rigid water column mode N°3, (iii) the downstream gallery elastic modes, see N° 4 and 5, (iv) the penstock elastic modes, see N°6 and 11, and (v) the upstream gallery elastic modes, see N°8 and 13. The mode shape obtained with the eigenvalue analysis corresponds fully to the mode shape identified from the time mode simulation and thus

confirms the nature of the phenomena of rigid and elastic water column mode. The mode shape and period of the upstream and downstream mass oscillations also fits well with the time domain simulation results of Fig. 6.

No	Eigen Value	Eigen Mode of Pressure	Period	Description	Scale
1	-0.001118 + j*0.028619	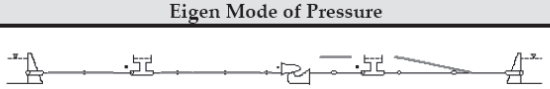	T=219s	Downstream Mass Oscillation	10
2	-0.002749 + j*0.041111		T=153s	Upstream Mass Oscillation	10
3	-0.164293 + j*0.528260		T=11.89s	Penstock Rigid Water Column Mode	1
4	-0.001342 + j*1.076944		T=5.83s	Downstream Gallery 1st Elastic Mode	1
5	-0.001228 + j*2.170392	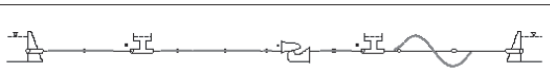	T=2.89s	Downstream Gallery 2nd Elastic Mode	1
6	-0.171264 + j*2.991849		T=2.10s	Penstock 1st Elastic Mode	1
8	-0.002786 + j*3.574846		T=1.76s	Upstream Gallery 1st Elastic Mode	1
11	-0.056142 + j*5.894269	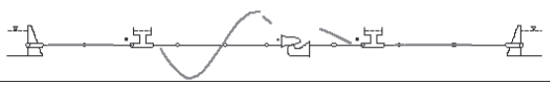	T=1.07s	Penstock 2nd Elastic Mode	1
13	-0.002772 + j*7.130790	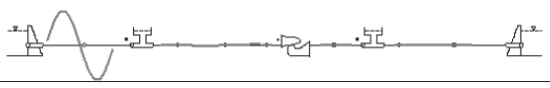	T=0.88s	Upstream Gallery 2nd Elastic Mode	1

Tab. 3 Pressure mode shape of the case study neglecting the second pump-turbine at time t=3.8s.

No	Eigen Value	Eigen Mode of Discharge	Period	Description	Scale
1	-0.001118 + j*0.028619	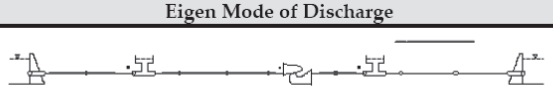	T=219s	Downstream Mass Oscillation	1
2	-0.002749 + j*0.041111	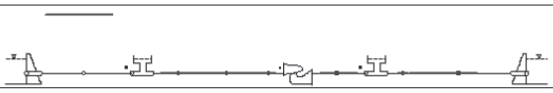	T=153s	Upstream Mass Oscillation	1
3	-0.164293 + j*0.528260	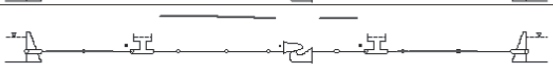	T=11.89s	Penstock Rigid Water Column Mode	1
4	-0.001342 + j*1.076944	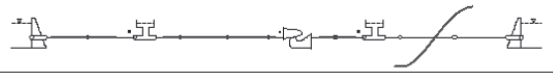	T=5.83s	Downstream Gallery 1st Elastic Mode	1
5	-0.001228 + j*2.170392	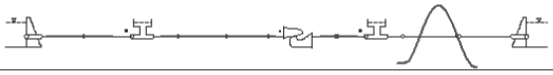	T=2.89s	Downstream Gallery 2nd Elastic Mode	1
6	-0.171264 + j*2.991849	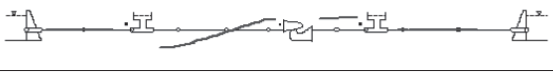	T=2.10s	Penstock 1st Elastic Mode	1
8	-0.002786 + j*3.574846	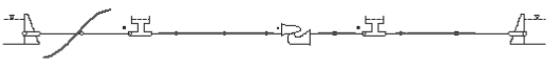	T=1.76s	Upstream Gallery 1st Elastic Mode	1
11	-0.056142 + j*5.894269	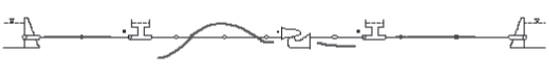	T=1.07s	Penstock 2nd Elastic Mode	1
13	-0.002772 + j*7.130790	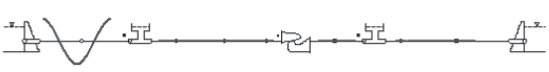	T=0.88s	Upstream Gallery 2nd Elastic Mode	1

Tab. 4 Discharge mode shape of the case study neglecting the second pump-turbine at time t=3.8s.

Eigenvalues during transient behavior

The complex eigenvalues related to the penstock elastic modes are computed during the transient behavior for the following times t=0s, 1s, 2.4s, 3.8s, 6.5s, 8.7s, 9.8s, 10.9s, 11.9s, 12.8s, 14.6s, 16.3s and 17.8s. The first eigenvalues related to the penstock elastic modes are represented in complex plan in Fig. 11. At time equal to t=0s, all real parts are negative and the eigenvalues are on left hand side of the complex plan, *i.e.* the modes are stable. For the time t=0s, the eigenvalues are computed assuming connection to the power network. Thus constant rotational speed is assumed and only variation of the pump-turbine head as function of the discharge is considered. Then, for time t=1s, the pump-turbine is disconnected from the power network, then rotational speed variations are possible. The eigenvalues are computed according to equation (7). The eigenvalues are only slightly influenced by the disconnection to the grid. Then, as the pump-turbine is reaching the runaway, the eigenvalues are moving from left hand side to right hand side of the complex plan, *i.e.* they change from stable to unstable modes. Then, during the rigid water column oscillation they are moving from left to right hand side back and forth.

It can be also noticed that the damping for the time t=1s of the penstock elastic modes, is strongly influenced by the relative position of the pump-turbine with respect to each mode shape [1]. Moreover, the penstock elastic modes feature much higher damping than the elastic modes of the upstream and downstream galleries due to the presence of the pump-turbine on the penstock. The fact that the eigenvalues are moving back and forth from stable to unstable regions also explains why the oscillation amplitudes are bounded. During the time the eigenvalue is on the right hand side of the complex plane, the amplitudes are amplified while they are damped when the eigenvalue is on the left hand side of the complex plane.

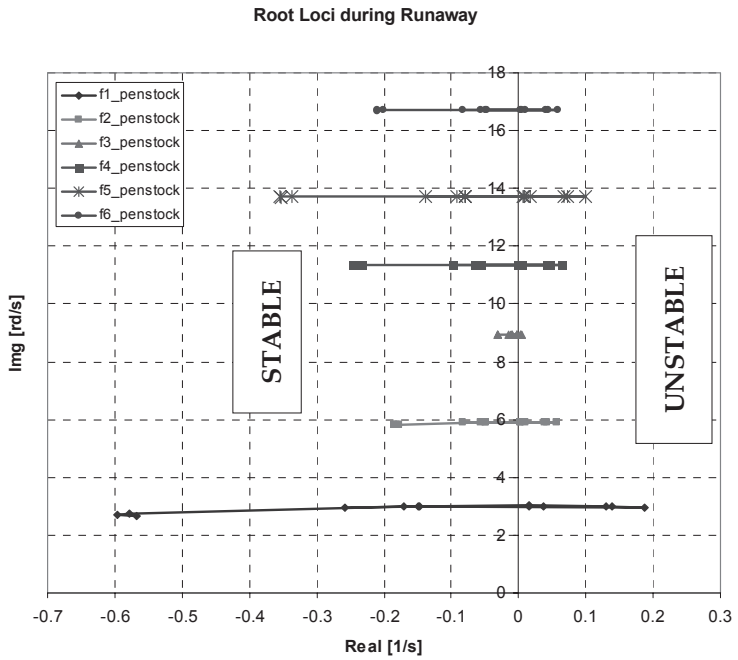

Fig. 11 Complex eigenvlaues of penstock elastic modes during transient.

In order to compare the stability of the rigid and elastic water column mode during the transient behavior of the pump-turbine, the related complex eigenvalues are presented in Fig. 12 left and their real part, *i.e.* the damping, is presented in Fig. 12 right. It can be noticed that the elastic mode features always a lower damping than the rigid mode. This explains why the elastic mode becomes dominant after 200s as the elastic mode is more unstable.

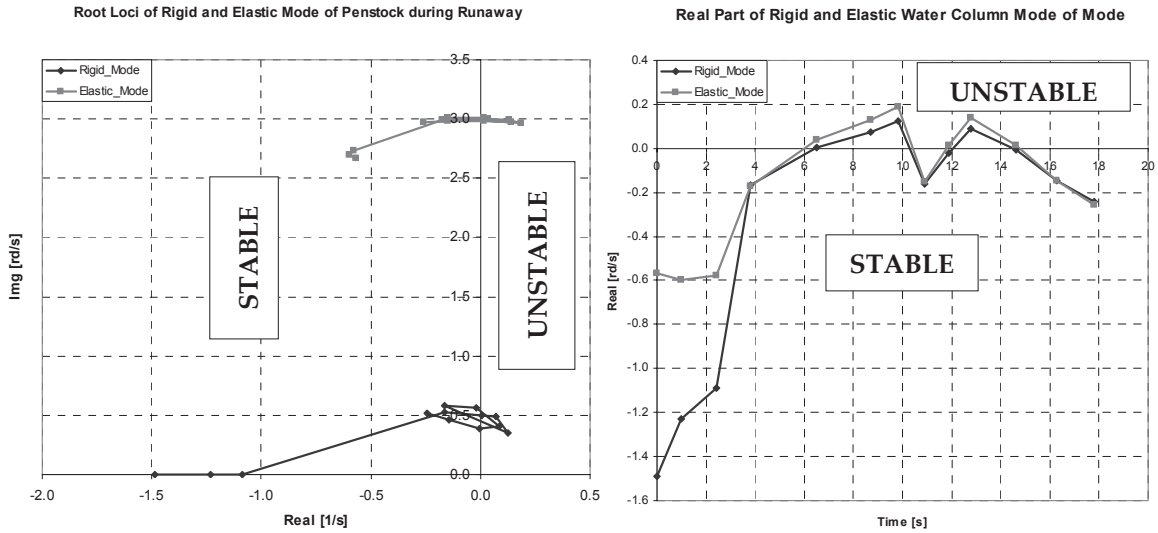

Fig. 12 Rigid and elastic water column mode eigenvalues during transient in complex plan (left) and real part as function of time (right).

Fig. 13 shows the transient operating point of the pump-turbine between t=0s and t=10.9s in the turbine characteristic Q11=Q11(N11) and T11=T11(N11). From Fig. 12, it can be noticed that both the elastic and rigid modes become unstable from about t=6s. This also corresponds to the time that the operating point experiences positive gradient in the turbine characteristic at runaway, as described by Martin [8]. Moreover, the real part of both modes becomes negative again between t=10 and 12s. As shown in Fig. 13, it corresponds to the moment when the operating point reaches negative slope in the lower part of the turbine characteristic illustrated at the time t=10.9s. The mean value of the period obtained from the eigenvalue analysis during the runaway between time=6.5s and time=17.8s is equal to T_{RW}=13.25s and corresponds very well to the analytical prediction of Martin [7] of equation (5).

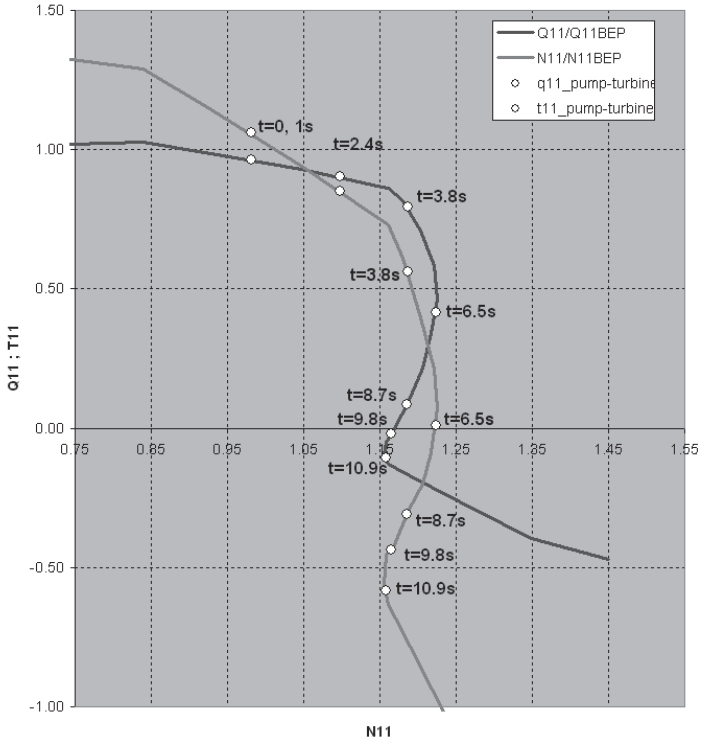

Fig. 13 Pump-turbine operating point during the runaway.

7 CONCLUSIONS

This paper presents the simulation of unstable operation of a pump-turbine resulting from servomotor failure during emergency shutdown. It is pointed out that first the pump-turbine experiences rigid water column mode characterized by high period of oscillation of 15 seconds and that after 250 seconds there is switch from rigid column mode to elastic column mode oscillation. The elastic water column mode represents huge risk for the safety of the power plant if it occurs at high guide vane openings as the peak-to-peak pressure amplitudes can reach 1.7 times the rated head, possibly at penstock locations not even designed for the maximum design head. This emphasizes the importance of the protection redundancy with main inlet valve closure and intake gate closure after emergency shutdown. Consequently, it would be recommended to check the switch time between rigid and elastic mode from simulation to ensure that all the protection valves would have closed before the switch could happen and jeopardize the power plant safety.

This system is also analyzed using new eigenvalues and eigenmodes module implemented in the software SIMSEN. The representation of the time evolution of the damping of both the rigid and elastic water column modes shows that the elastic mode is more unstable than the rigid mode, and therefore becomes dominant after 250s. It also shows that the unstable behavior is induced by positive gradients of the pump-turbine characteristic as it was already demonstrated by Martin [8].

8 NOMENCLATURE

A: pipe cross section [m^2]
A_g: gallery cross section [m^2]
A_{ST}: surge tank cross section [m^2]
D_{ref}: machine reference diameter [m]
H: net head [m]
Q: discharge [m^3/s]
N: rotational speed [rpm]
P: power [W]
T: Torque [Nm]
a: pipe wave speed [m/s]
h: piezometric head $h=z+p/(\rho g)$ [m]
g: gravity [m/s^2]
p: static pressure [Pa]
l_g: length of the gallery [m]
p: pressure [Pa]
t: time [s]
x: position [m]
y: turbine guide vane opening [-]
Z: elevation above a datum [m]
ν: specific speed $\nu = \omega_R (Q_R / \pi)^{1/2} / (2 \cdot g \cdot H_R)^{3/4}$ [-]
ω: rotational pulsation [rd/s]
R: subscript for rated

9 ACKNOWLEDGMENT

The authors would like to thankful Mr. Philippe Allenbach from Laboratory of Electrical machines from EPFL, for his important contribution in the development of the eigenvalue module of SIMSEN. For this paper, the authors took advantages of the development of the SIMSEN hydraulic extension, developed with the financial support of: CTI, Swiss Federal Commission for Technology and Innovation, contract awards No 5750.1 EBS, EOS, BKW FMB Energie AG, SIG, SIL, Groupe E, Electricité Suisse and PSEL Funds for Projects and Studies of the Swiss Electric Utilities, contract awards No 215 Scapin. The authors also would like to thank EDF-CIH, VOITH Hydro and ALSTOM Power Hydro (CTI project 8330) for their financial support and their scientific contribution in the development of the hydraulic extension of SIMSEN.

10 REFERENCES

[1] Alligné, S., Nicolet, C., Allenbach, P. , Kawkabani, B. , Simond, J.-J., Avellan, F., *Influence of the Vortex Rope Location of a Francis Turbine on the Hydraulic System Stability*, Proceedings of the 24th IAHR Symposium on Hydraulic Machinery and Systems, Foz do Iguassu, Brazil, October 27 -31, 2008, paper 106.

[2] Brekke, H., Xin-Xin, L., *The structure matrix with amplitude-frequency dependent frictional damping*, Société Hydrotechnique de France, Proc. XXe Journée de l'Hydraulique, Lyon, 4-6 avril 1989, Question N°III, Rapport N°1.

[3] Dörfler, P. K., Engineer, A. J., Pendse, R. N., Huvet, P., and Brahme, M. V., *Stable operation achieved on single-stage reversible pump-turbine showing instability at no-load,* In Proceeding of the 19th IAHR Symposium on Hydraulic Machinery and Systems (Singapore, 1998), pp. 430–440.

[4] Huvet, P., *Steady oscillation between pump-turbine operating at partial flow and surge shaft*, In Proc. 16th Symposium of the IAHR, Sao Paola, Brazil, 1992.

[5] Jaeger, R. C., *Fluid transients in hydro-electric engineering practice* ".Glasgow: Blackie, 1977.

[6] Liu, X., Liu, C., *Eigenanalysis of Oscillatory Instability of a Hydropower Plant Incuding Water Conduit Dynamics*, In IEEE Transactions on Power Systems, vol. 22, No. 2, 2007.

[7] Martin, C. S., *Stability of pump-turbines during transient operation*. In Proceedings of the 5th Int. Conf. on Pressure Surges (Hannover, Germany, 1986), pp. 61–71. paper C3.

[8] Martin, C. S., *Instability of pump-turbines with s-shaped characteristics*. In Proceeding of the 20th IAHR Symposium on Hydraulic Machinery and Systems (Charlotte, USA, 2000).

[9] Nicolet, C., *Hydroacoustic modelling and numerical simulation of unsteady operation of hydroelectric systems*, Thesis EPFL n° 3751, 2007, (http://library.epfl.ch/theses/?nr=3751).

[10] Nicolet, C., Alligné, S., Kawkabani, B. , Simond, J.-J., Avellan, F., *Unstable Operation of Francis Pump-Turbine at Runaway: Rigid and Elastic Water Column Oscillation Modes*, Proceedings of the 24th IAHR Symposium on Hydraulic Machinery and Systems, Foz do Iguassu, Brazil, October 27 -31, 2008, paper 150.

[11] Paynter, H. M., *Surge and water hammer problems*. Transaction of ASCE, vol. 146, p 962-1009, 1953.

[12] Pejovic, S., Krsmanovic, L., Jemcov, R., Crnkovic, P., *Unstable operation of high-head reversible Pump-Turbines*. In Proceeding of the 8th IAHR Symposium on Hydraulic Machinery and Systems, Leningrad, pp. 283-295.

[13] Taulan, J. P. *Pressure surges in hydroelectric installations – Peculiar effects of low specific speed turbine characteristics*. Proc. 4th BHRA Int. Conf. on Pressure Surges, Bath, 1983, Paper H2, pp. 337-351.

[14] Sapin, A., *Logiciel modulaire pour la simulation et l'étude des systèmes d'entraînement et des réseaux électriques*, Thesis EPFL n° 1346, 1995, (http://library.epfl.ch/theses/?nr=1346).

[15] Souza, O.H., Jr.; Barbieri, N.; Santos, A.H.M.; *Study of hydraulic transients in hydropower plants through simulation of nonlinear model of penstock and hydraulic turbine model*" IEEE Transactions on Power Systems, vol. 14, issue 4, pp. 1269 – 1272, 1999.

[16] Wylie, E. B. & Streeter, V.L., Fluid transients in systems. Prentice Hall, Englewood Cliffs, N.J, 1993.